Neuron, Volume *79*

Supplemental Information

Intersecting Circuits Generate Precisely Patterned Retinal Waves

Alejandro Akrouh and Daniel Kerschensteiner

Inventory of Supplemental Information

Figure S1

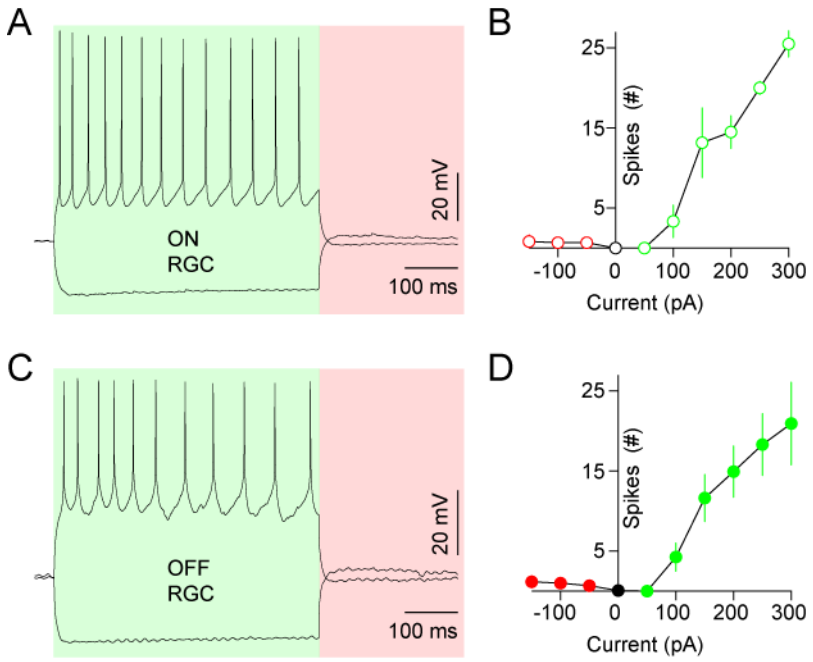

Figure S1. Intrinsic excitability of ON and OFF RGCs at P11-13 (related to Figure 1)

(A) Responses of a representative ON RGC to 500-ms long de- (I = 150 pA) and hyperpolarizing (I = -150 pA) current injections. (B) Average number of spikes (± SEM, n = 3) triggered by varying currents. For depolarizing pulses, spikes were counted during the current injections (green-shaded area in A). For hyperpolarizing currents, spikes were counted in the segment following the current pulse (red-shaded area in A). (C) Responses of an OFF RGC to somatic current injections (150 pA, - 150 pA). (D) Population data (n = 7) of OFF RGCs analyzed as in (B).

Figure S2

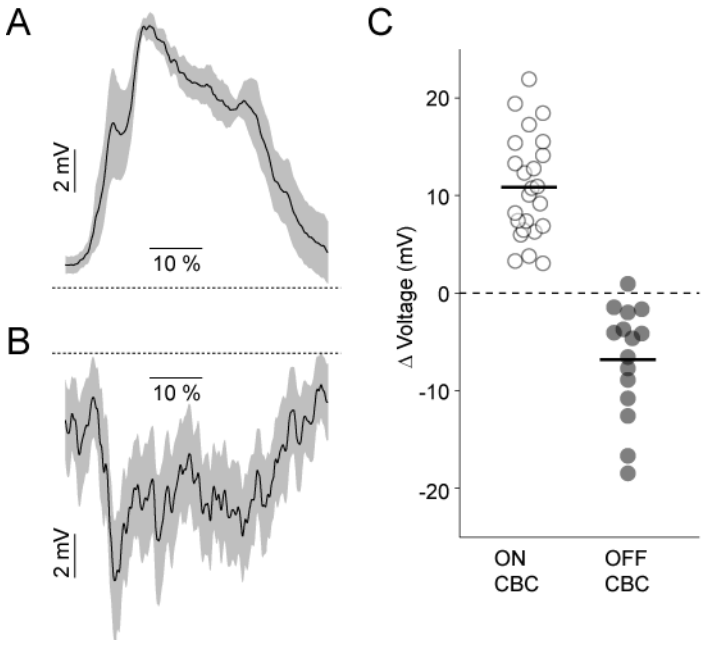

Figure S2. CBC voltage fluctuations during waves identified in RGC recordings (related to Figure 2)

(A, B) Average (± SEM) voltage traces of representative ON (A) and OFF (B) CBCs during waves detected in simultaneously measured EPSCs of ON RGCs (or IPSCs in OFF RGCs). Because the duration of waves varies, traces were resampled and aligned, and time is expressed as a percentage of the total duration. (C) The mean of the maximal voltage changes during each wave of each CBC is shown by circles (open - ON, filled - OFF). Horizontal lines indicate population averages.

Figure S3

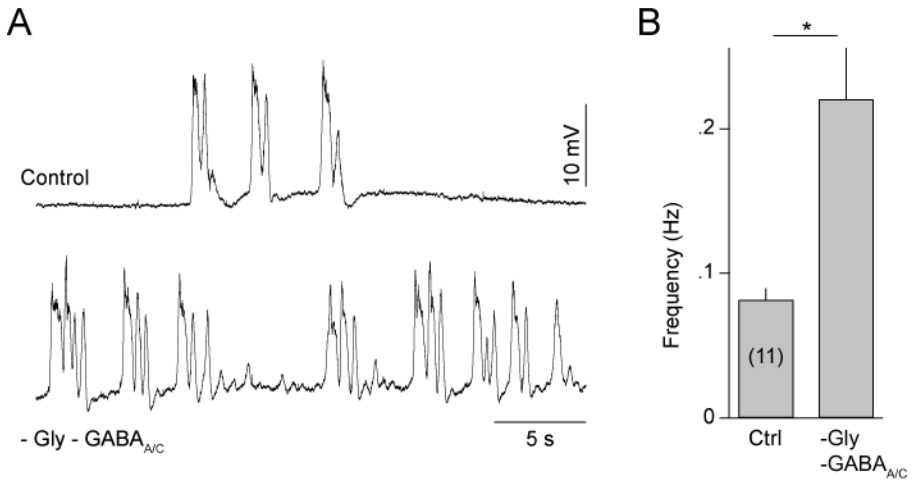

Figure S3. Blockade of GABA- and glycinergic transmission increases the frequency of stage III waves in CBCs (related to Figure 3)

(A) Representative current-clamp recording from an ON CBC in control solutions (*top trace*) and in the presence of strychnine (500 nM), gabazine (5 μM) and TPMPA (50 μM) (*bottom trace*). (B) Group data (mean ± SEM) of the frequency of waves in CBCs in control (Ctrl) conditions and during blockade of inhibitory neurotransmission (-Gly, -GABA$_{A/C}$). The number of CBCs included in this analysis is shown in brackets.

Figure S4

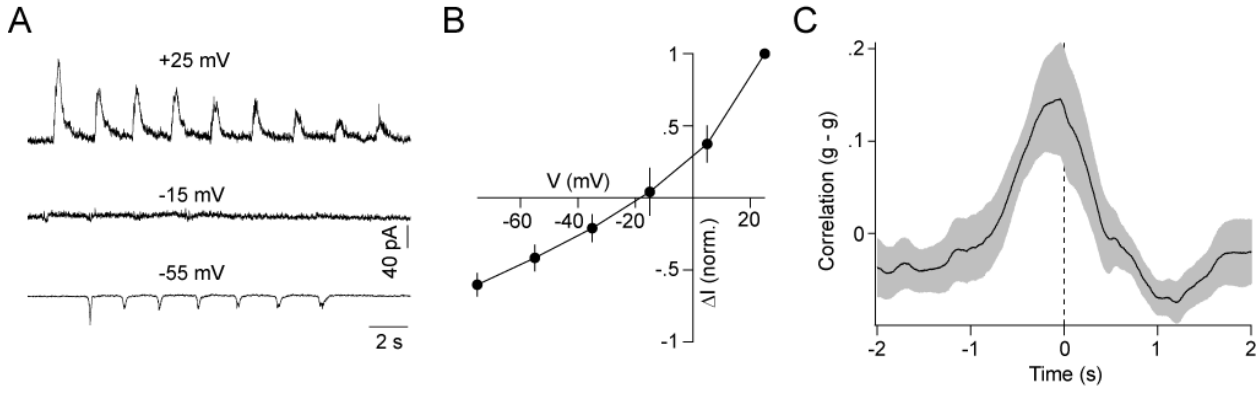

Figure S4. OFF CBCs receive excitatory input during the ON phase of stage III waves via cation-nonselective conductances (related to Figure 3)

(A) Voltage-clamp traces of a representative OFF CBC recorded in the presence of strychnine (500 nM), gabazine (5 μM) and TPMPA (50 μM) at a series of holding potentials. (B) Normalized I-V relationship (mean ± SEM, n = 4) of wave-associated input currents to OFF CBCs during blockade of inhibitory synaptic transmission. (C) Crosscorrelation of EPSCs recorded simultaneously in OFF CBCs and ON RGCs in control conditions (PT: -67 ± 85 ms, n = 5).

Figure S5

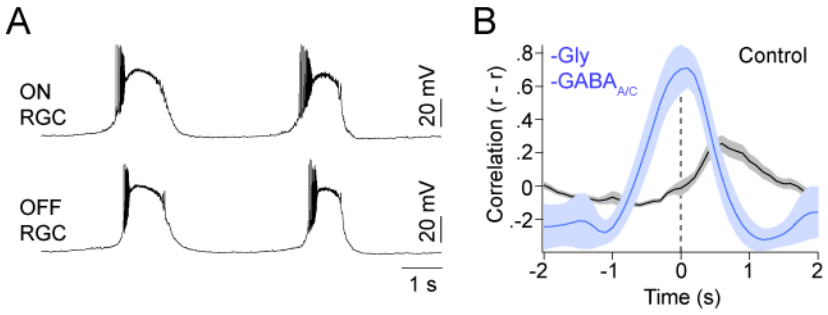

Figure S5 Blockade of crossover inhibition synchronizes ON and OFF RGC spiking (related to Figure 5)

(A) Simultaneous current-clamp recording of an ON and OFF RGC in the presence of strychnine (500 nM), gabazine (5 μM) and TPMPA (50 μM) (D) Crosscorrelation of the spike rate (r) of ON and OFF RGCs (mean ± SEM, Control: n = 11, -Gly -GABA$_{A/C}$: n = 5) in control conditions (black) and in the presence of glycinergic- and GABAergic blockers (blue). Some RGCs entered depolarization block during waves in the presence of inhibitory blockers. For these cells crosscorrelations were calculated on low-pass (< 50 Hz) filtered voltage traces rather than spike trains.

Figure S6

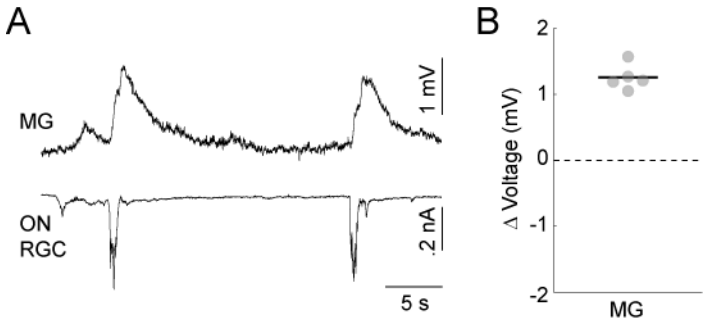

Figure S6. Müller glia depolarize during stage III waves (related to Figure 5)

(A) Representative traces of simultaneous current- and voltage-clamp (EPSC, V_M ~ -60 mV) recordings from an MG and ON RGC, respectively. Circles show the average amplitude of wave-associated voltage deflections observed in MGs. Line indicates the mean of the population.

Figure S7

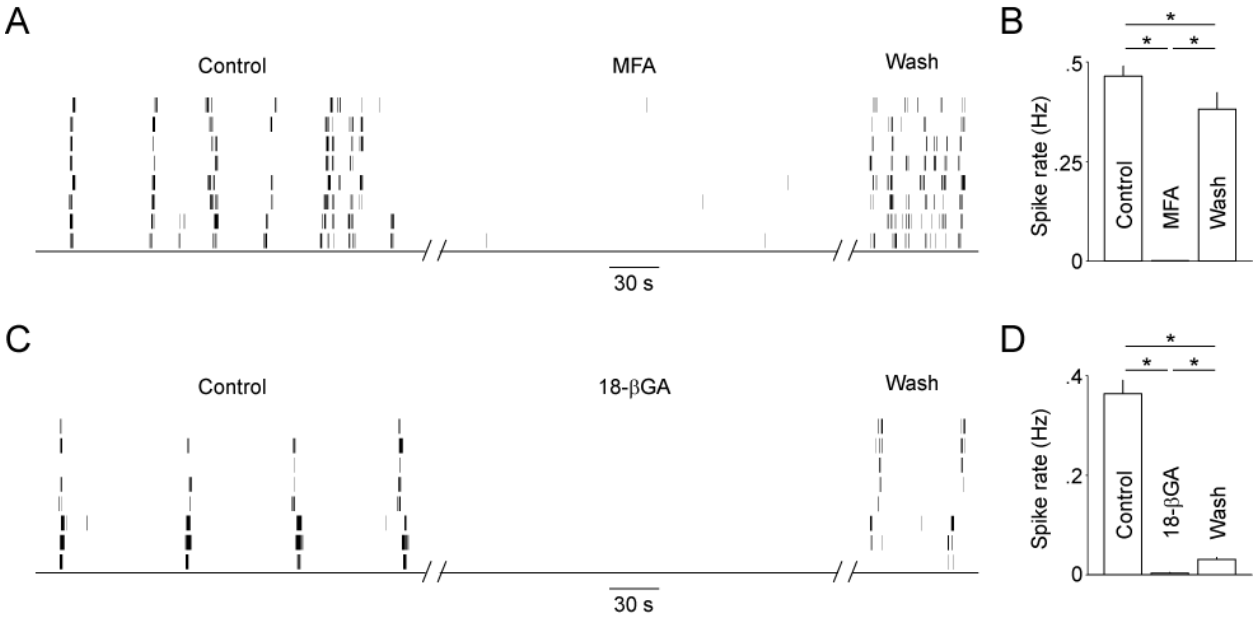

Figure S7. Meclofenamic acid and 18-β-Glycyrrhetinic acid reversibly silence stage III waves in MEA recordings (related to Figure 7)

(A) Raster plots of RGC spike trains recorded in mACSF (Control), in the presence of MFA (200 μM) and following its washout. (B) Summary data of RGC spike rates under these conditions (mean ± SEM, n = 391 cells from 4 retinas). (C) Representative RGC spike trains recorded in mACSF, in the presence of 18-βGA (50 μM) and after washout of the drug (> 2 hrs). (D) Group data of RGC spike rates in these conditions (mean ± SEM, n = 187 cells from 2 retinas).

Supplemental Discussion

An interesting question is how the return to baseline voltage without appreciable overshoot (Figure 2) that we observe in OFF CBCs leads to a phasic EPSC in OFF RGCs. The most parsimonious explanation is that between waves, when OFF CBCs are depolarized, synapses between OFF CBCs and OFF RGCs are depressed and transiently recover during wave-associated hyperpolarizations (Wan and Heidelberger, 2011). Several mechanisms could contribute to synaptic depression and recovery. Presynaptic voltage-gated L- and T-type Ca^{2+} channels could be inactivated and recover between and during waves, respectively (Berntson et al., 2003; de la Villa et al., 1998; Pan, 2000; Pan et al., 2001). However, Ca^{2+} influx associated with channel recovery would be expected to generate rebound depolarizations in OFF CBCs, which we did not observe. We therefore favor a model in which the pool of readily releasable vesicles in OFF CBC axon terminals is depleted between waves and replenished during ON phase hyperpolarizations. Rapid bidirectional changes in vesicle pool occupancy have been observed at CBC ribbon synapses in mature circuits (Burrone and Lagnado, 2000; Mennerick and Matthews, 1996; Singer and Diamond, 2003, 2006) where they mediate adaptive computations (Dunn and Rieke, 2008; Jarsky et al., 2011; Manookin and Demb, 2006; Oesch and Diamond, 2011). Desensitization of postsynaptic AMPARs (Lukasiewicz et al., 1995; Matsui et al., 1998) and activation of presynaptic mGluRs (Quraishi et al., 2007) may accentuate the transience of OFF RGC responses and contribute to synaptic depression between waves, though both mechanisms appear to play only a modest role in shaping light-evoked EPSCs (Awatramani and Slaughter, 2001; Lukasiewicz et al., 1995).

Supplemental Experimental Procedures

Imaging

BCs, ACs and MGs recorded in the INL were distinguished based on their morphology as follows. Each BC had a primary dendrite oriented towards the outer retina and a single axon stalk that crossed through the INL before branching within a narrow stratum in the IPL. RBCs were distinguished from CBCs by their smaller axon arbors and stratification close to RGC somata (Ghosh et al., 2004; Kerschensteiner et al., 2009). AC types differ widely in their morphology, but generally have several primary processes emanating from their somata towards the IPL and no neurites oriented towards the outer retina (MacNeil and Masland, 1998). The lateral extent of narrowly stratified arbors of wide-field ACs is much greater than that of BCs, and the arbors of most medium- to narrow-field ACs, unlike BCs, target multiple strata within the IPL (Menger et al., 1998). MGs have a prominent endfeet forming the ILM and small lateral branches throughout the inner and outer plexiform layers (OPL) of the retina (Cajal, 1972).

Supplemental References

Awatramani, G.B., and Slaughter, M.M. (2001). Intensity-dependent, rapid activation of presynaptic metabotropic glutamate receptors at a central synapse. J Neurosci 21, 741-749.

Berntson, A., Taylor, W.R., and Morgans, C.W. (2003). Molecular identity, synaptic localization, and physiology of calcium channels in retinal bipolar cells. Journal of neuroscience research 71, 146-151.

Burrone, J., and Lagnado, L. (2000). Synaptic depression and the kinetics of exocytosis in retinal bipolar cells. J Neurosci 20, 568-578.

Cajal, S.R. (1972). The structure of the retina (Charles C. Thomas).

de la Villa, P., Vaquero, C.F., and Kaneko, A. (1998). Two types of calcium currents of the mouse bipolar cells recorded in the retinal slice preparation. Eur J Neurosci 10, 317-323.

Dunn, F.A., and Rieke, F. (2008). Single-photon absorptions evoke synaptic depression in the retina to extend the operational range of rod vision. Neuron 57, 894-904.

Ghosh, K.K., Bujan, S., Haverkamp, S., Feigenspan, A., and Wassle, H. (2004). Types of bipolar cells in the mouse retina. J Comp Neurol 469, 70-82.

Jarsky, T., Cembrowski, M., Logan, S.M., Kath, W.L., Riecke, H., Demb, J.B., and Singer, J.H. (2011). A synaptic mechanism for retinal adaptation to luminance and contrast. J Neurosci 31, 11003-11015.

Kerschensteiner, D., Morgan, J.L., Parker, E.D., Lewis, R.M., and Wong, R.O. (2009). Neurotransmission selectively regulates synapse formation in parallel circuits in vivo. Nature 460, 1016-1020.

Lukasiewicz, P.D., Lawrence, J.E., and Valentino, T.L. (1995). Desensitizing glutamate receptors shape excitatory synaptic inputs to tiger salamander retinal ganglion cells. J Neurosci 15, 6189-6199.

MacNeil, M.A., and Masland, R.H. (1998). Extreme diversity among amacrine cells: implications for function. Neuron 20, 971-982.

Manookin, M.B., and Demb, J.B. (2006). Presynaptic mechanism for slow contrast adaptation in mammalian retinal ganglion cells. Neuron 50, 453-464.

Matsui, K., Hosoi, N., and Tachibana, M. (1998). Excitatory synaptic transmission in the inner retina: paired recordings of bipolar cells and neurons of the ganglion cell layer. J Neurosci 18, 4500-4510.

Menger, N., Pow, D.V., and Wassle, H. (1998). Glycinergic amacrine cells of the rat retina. J Comp Neurol 401, 34-46.

Mennerick, S., and Matthews, G. (1996). Ultrafast exocytosis elicited by calcium current in synaptic terminals of retinal bipolar neurons. Neuron 17, 1241-1249.

Oesch, N.W., and Diamond, J.S. (2011). Ribbon synapses compute temporal contrast and encode luminance in retinal rod bipolar cells. Nat Neurosci 14, 1555-1561.

Pan, Z.H. (2000). Differential expression of high- and two types of low-voltage-activated calcium currents in rod and cone bipolar cells of the rat retina. J Neurophysiol 83, 513-527.

Pan, Z.H., Hu, H.J., Perring, P., and Andrade, R. (2001). T-type Ca(2+) channels mediate neurotransmitter release in retinal bipolar cells. Neuron 32, 89-98.

Quraishi, S., Gayet, J., Morgans, C.W., and Duvoisin, R.M. (2007). Distribution of group-III metabotropic glutamate receptors in the retina. J Comp Neurol 501, 931-943.

Singer, J.H., and Diamond, J.S. (2003). Sustained Ca2+ entry elicits transient postsynaptic currents at a retinal ribbon synapse. J Neurosci 23, 10923-10933.

Singer, J.H., and Diamond, J.S. (2006). Vesicle depletion and synaptic depression at a mammalian ribbon synapse. J Neurophysiol 95, 3191-3198.

Wan, Q.F., and Heidelberger, R. (2011). Synaptic release at mammalian bipolar cell terminals. Vis Neurosci 28, 109-119.